Efficient Self-Propelling of Small-Scale Condensed Microdrops by Closely Packed ZnO Nanoneedles

ARTICLE *in* JOURNAL OF PHYSICAL CHEMISTRY LETTERS · MAY 2014

Impact Factor: 7.46 · DOI: 10.1021/jz500798m

6 AUTHORS, INCLUDING:

Jian Tian
Shanghai Institute of Applied Physics
4 PUBLICATIONS **38** CITATIONS
SEE PROFILE

Juan Li
Chinese Academy of Sciences
65 PUBLICATIONS **768** CITATIONS
SEE PROFILE

Xi-Qiao Feng
Tsinghua University
330 PUBLICATIONS **5,504** CITATIONS
SEE PROFILE

Xuefeng Gao
Chinese Academy of Sciences
34 PUBLICATIONS **3,601** CITATIONS
SEE PROFILE

THE JOURNAL OF PHYSICAL CHEMISTRY Letters

Letter

pubs.acs.org/JPCL

Efficient Self-Propelling of Small-Scale Condensed Microdrops by Closely Packed ZnO Nanoneedles

Jian Tian,[†,¶] Jie Zhu,[†] Hao-Yuan Guo,[‡] Juan Li,[†] Xi-Qiao Feng,[‡] and Xuefeng Gao*[,†]

[†]Advanced Thermal Nanomaterials and Devices Research Group, Nanobionic Division, Suzhou Institute of Nano-Tech and Nano-Bionics, Chinese Academy of Sciences, Suzhou 215123, People's Republic of China

[‡]Department of Engineering Mechanics, Tsinghua University, Beijing 100084, People's Republic of China

[¶]University of Chinese Academy of Sciences, Chinese Academy of Sciences, Beijing 100049, People's Republic of China

Supporting Information

ABSTRACT: Realizing the efficient self-propelling of small-scale condensed microdrops is very challenging but extremely important to design and develop advanced condensation heat transfer nanomaterials and devices, for example, for power generation and thermal management. Here, we present the efficient self-propelling of small-scale condensed microdrops on the surface of closely packed ZnO nanoneedles, as-synthesized by facile, rapid, and inexpensive wet chemical crystal growth followed by hydrophobic modification. Compared with flat surfaces, the nanostructured surfaces with the same low-surface-energy chemistry possess far higher time-averaged density of condensed droplets at the microscale, among which those with diameters below 10 μm occupy more than 80% of the total drop number of residual condensates. Theoretical analyses clearly reveal that this remarkable property should be ascribed to the extremely low solid−liquid adhesion of the surface nanostructure, where excess surface energy released from the coalescence of smaller condensed microdrops can be sufficient to ensure the self-propelled jumping of merged microdrops.

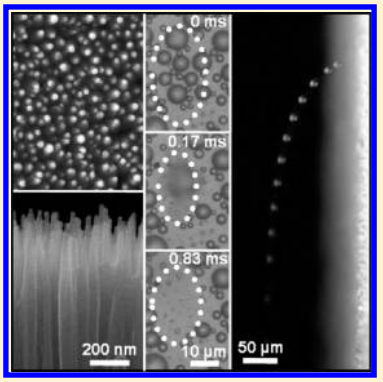

SECTION: Surfaces, Interfaces, Porous Materials, and Catalysis

Condensed microdrop self-propelling surfaces have attracted great interest due to their values in basic research and technological innovations, for example, enhancing condensation heat transfer for high-efficiency power generation and thermal management.[1−3] The self-propelling of condensed microdrops on the nanostructured surfaces can be realized by excess surface energy released from their mutual coalescence without requiring external forces such as gravity and steam shear force.[4] In principle, the self-propelling of condensed microdrops can reduce heat resistance and increase renewal frequency (performing more cycles of nucleation, growth, and departure per unit area), which is useful to enhance the total dropwise condensation heat transfer performance.[3] Recently, great breakthrough has been made in realizing the self-propelling of condensed microdrops with random diameter distribution from tens to hundreds of micrometers by different materials of nanostructures[5−13] and hierarchical structures[4,14−17] modified with low-surface-energy chemicals. Compared with the costly top-down nanofabrication methods,[4−7,14,15] the bottom-up wet chemical nanosynthesis methods[8−13,17] show obvious advantages in low-cost large-area processing and equipment accessibility. However, it is still a great challenge to realize the high-efficiency self-propelling of small-scale (e.g., <10 μm) condensed microdrops at this stage. Thus, it is significant to explore innovative interfacial nanomaterials with the high-efficiency self-propelling ability of small-scale condensed microdrops using wet chemical methods and their structure−property relationships.

Here, we report a type of closely packed zinc oxide (ZnO) nanoneedles with high-efficiency self-propelling ability of small-scale condensed microdrops, which are achieved by facile, rapid, and cheap wet chemical crystal growth and hydrophobic treatment. Compared to the flat samples, our samples have far higher time-averaged density of condensed droplets at the microscale, especially below 10 μm with a drop number distribution of more than 80%, which is apparently higher than the previously reported cases. The remarkable property is ascribed to the minimal solid−liquid adhesion of closely packed ZnO nanoneedles, where excess surface energy released from the coalescence of smaller microdrops can be sufficient to drive the self-propelling of merged microdrops. These findings are very significant to develop high-efficiency condensation heat transfer nanomaterials and devices.

Figure 1 shows the typical scanning electron microscopic (SEM) top view and side view of the as-synthesized ZnO nanoneedles, which can be obtained by immersing seed-coated glass slides in the aqueous solution of isopyknic 0.5 mol L^{-1} zinc nitrate hexahydrate and 4 mol L^{-1} sodium hydroxide at 60

Received: April 22, 2014
Accepted: May 28, 2014

   dx.doi.org/10.1021/jz500798m | J. Phys. Chem. Lett. 2014, 5, 2084−2088

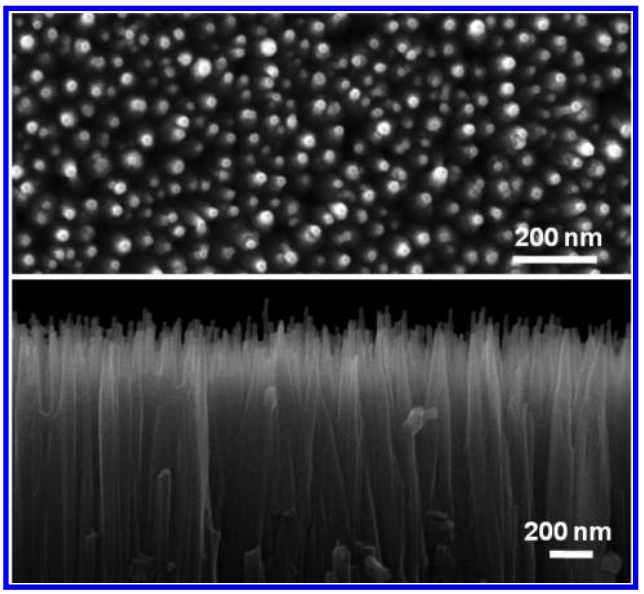

Figure 1. SEM top view (top) and side view (bottom) of the as-synthesized ZnO nanoneedles.

°C for 30 min (see the Experimental Methods section). These self-standing ZnO nanoneedles are arranged in a closely packed way, having the characteristic interspace (p) of 60 ± 17.1 nm, top diameter (d_t) of 20.3 ± 4.8 nm, end diameter of 98.3 ± 5.5 nm, and height of 2.85 ± 0.14 μm. The controllable synthesis of tapered nanoneedles with minimized top areas is based on the principle of diffusion-limited wet chemical crystal growth in a strong alkali system, where zinc ions can be rapidly consumed by violent reactions in the bulk to offer the chance of adjusting the diffusion rate of growth units transported to crystal facets at a proper growth condition of reaction temperature, time, and concentration.[18] Accordingly, we can easily obtain large-area ZnO nanoneedle films in a short duration.

Our experiments demonstrate that the as-synthesized nanostructured surfaces own a remarkable condensed microdrop self-propelling property after modifying low-surface-energy fluorosilane molecules. Figure 2a and b shows distinct dropwise condensation behavior of the nanostructured surface and the contrast flat surface, which are taken at the substrate temperature of 1 °C, ambient temperature of ∼25 °C, and relative humidity of ∼90%. It is evident that condensates on the nanostructured surface can continuously emerge, grow, and self-departure, always keeping their sizes at the micrometer scale (Figure 2a). With the time extending, the drop number density of condensates presents a first decreasing and then fluctuating trend. In contrast, condensates on the flat surface can continuously grow, accompanied by their sizes increasing from the micrometer scale to the millimeter (Figure 2b), and only can slide off under gravity as their diameters reach the capillary length (see Supporting Information Figure S1). No doubt that the aligned nanoneedles can dramatically reduce the residence durations and diameters of condensed droplets through self-departure.

To better offer insight into the self-propelling phenomena of condensates at the microscale, we investigate their details using high-speed, high-resolution three-dimensional optical microscopic imaging technology (Keyence VW-9000). Figure 2c shows representative optical top views of the self-departure instant of several small-scale condensed microdrops on the surface of vertically placed nanostructured samples. The jumping events are realized by the in-plane coalescence of adjacent quasi-static microdrops, which is implemented by their respective growth due to preferential condensation of ambient vapor on the surface of microdrops.[19] As shown in Figure 2d, the merged microdrop can eject from the nanostructured surface and then fall along a parabolic trajectory. It should be

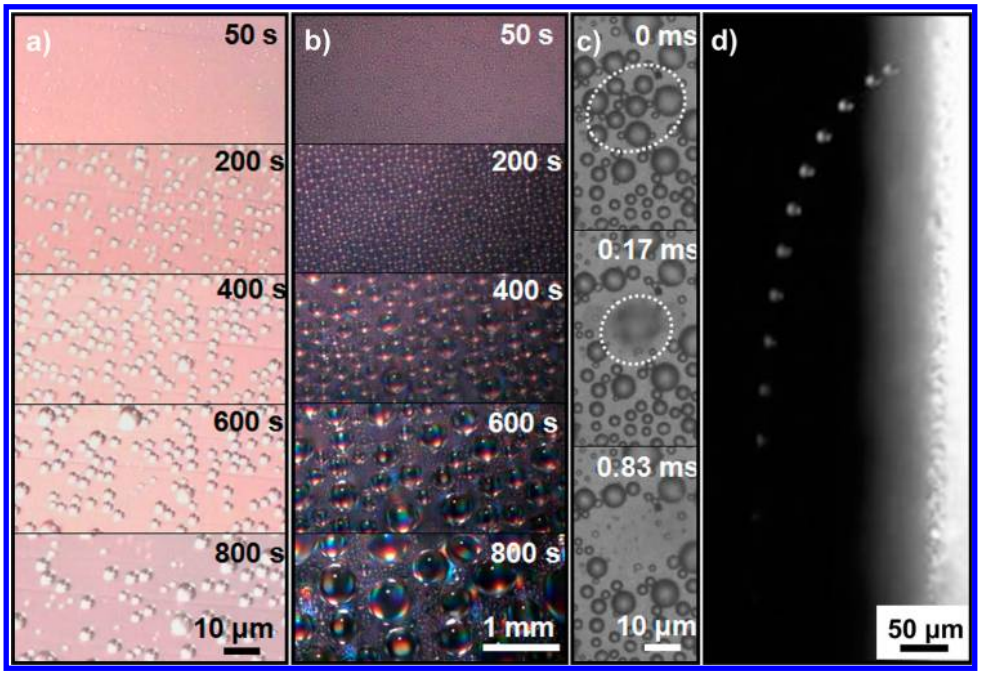

Figure 2. Time-lapse optical images showing distinct dropwise condensation behaviors of the nanostructured surface (a) and the contrast flat surface (b). Optical top views (c) and side view (d) showing the typical coalescence-induced self-propelling details of condensed microdrops on the nanostructured surface. All images are taken on the vertically placed sample surfaces.

dx.doi.org/10.1021/jz500798m | J. Phys. Chem. Lett. 2014, 5, 2084−2088

pointed out that for the horizontally placed nanostructured samples, the ejected microdrops can fall back to the sample surface and trigger the new dynamic impact-induced coalescence events, resulting in continuously coalescence-induced jumping events (see Supporting Information Figure S2), with their diameters scaling up from micrometers to submillimeters. In fact, the continuous jumping events are nonexistent for the vertically placed nanostructured samples because the ejected microdrops no longer fall on their surface.

To quantify and highlight the intrinsic dropwise condensation performance of our nanosamples at the microscale, we further analyze the drop number distribution of residence microdrops with diameters (d) of <10, 10−50, and 50−100 μm (Figure 3). Here, the corresponding statistic analyses are

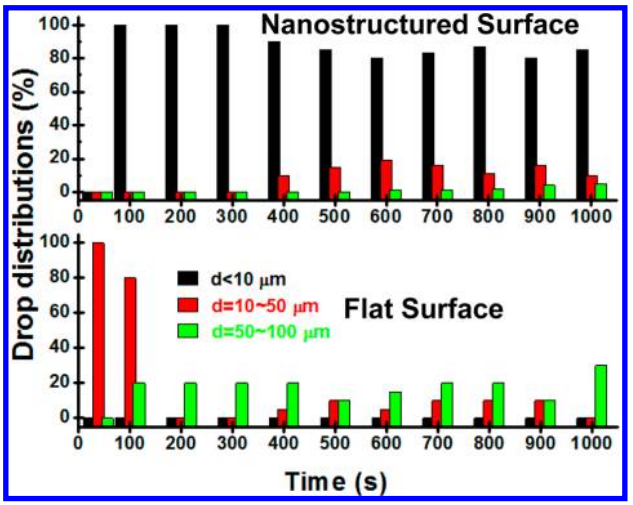

Figure 3. Drop number distribution of condensed microdrops with diameters (d) of <10, 10−50, and 50−100 μm on the vertically placed nanostructured samples (top) and contrast flat samples (bottom) varied with time.

collected from the vertically placed nanosamples to avoid disturbance from falling microdrops. Clearly, condensates with d < 10 μm can dominate on the nanostructured surface and present the slight fluctuation with the time extending; condensates with d = 10−50 μm can stably form only after 400 s, occupying 10−20%; and condensates with d > 50 μm can form only after ∼500 s, where their maximum fraction is not more than 10%. In contrast, the sizes of condensates on the flat surface can rapidly increase over 100 μm during very short duration (e.g., 200 s). Besides, condensates with sizes from the micrometer size to the millimeter cannot jump on the flat surface even after mutual coalescence (see Supporting Information Figure S1). Compared with the contrast flat surfaces, the aligned nanoneedle films can efficiently control the sizes of condensates at the microscale, especially below 10 μm, in which the drop number distribution is larger than 80% during the whole condensation process. It should also be pointed out that, compared with the previously reported cases presenting similar data descriptions,[4,10−12,14−17,20] our nanostructured samples possess the apparently higher time-averaged density of small-scale condensed microdrops, to the best of our knowledge.

In principle, the self-propelling dynamics of merged microdrops is governed by the balance of released surface energy (E_s), kinetic energy (E_k), viscous flow-induced dissipation energy (E_{vis}), and interfacial adhesion-induced dissipation energy (E_{int}), obeying the expression $E_k = E_s - E_{vis} - E_{int}$.[20−22] The gravitational potential energy may be neglected for the condensed microdrops with diameters far smaller than the capillary length $(\sigma_{LV}/\rho g)^{0.5} \approx 2.7$ mm, where σ_{LV} is the liquid−vapor interface tension (0.075 N m^{-1} at 5 °C). To simplify theoretical analysis, we only consider the merged case of two static microdrops with the same diameter (D) and apparent contact angle (α) as a model (note that this analysis method is also applicable to the coalescence process of multiple condensed microdrops after modification). As shown in Figure 4a, the quasi-static condensed microdrops can

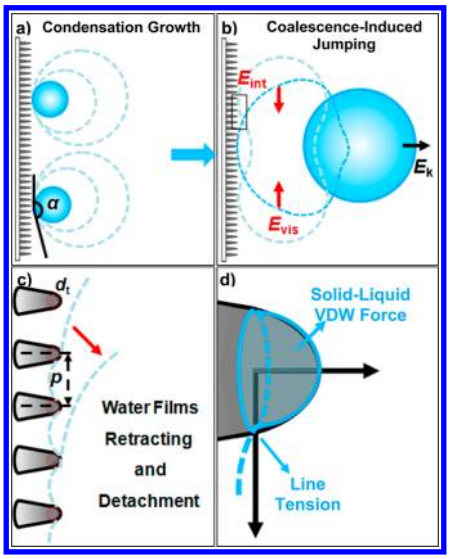

Figure 4. Schematics of the self-propelling mechanism of small-scale condensed microdrops on the top of closely packed nanoneedles. (a) Condensation growth of two microdrops, in the mode of constant contact angle (α), until closing to each other. (b) Self-propelled jumping of the merged microdrop. Here, $E_k = E_s - E_{vis} - E_{int} > 0$, where E_k is the kinetic energy of the jumping microdrop, E_s the released surface energy, E_{vis} the viscous flow-induced energy dissipation, and E_{int} the interfacial adhesion-induced energy dissipation. (c) A magnified image (corresponding to the black rectangle in panel b) showing the retracting and detaching process of water films on the top of nanoneedles (with a characteristic top diameter of d_t and interspace of p) in the coalescence-induced jumping instant. (d) Schematic of the top of a single nanoneedle contacting with water, where surface adhesion comes from solid−liquid van der Waals attraction and line tension.

gradually grow until closing to each other. Once the merging event occurs (Figure 4b), the excess surface energy would release, following $E_s \approx \sigma_{LV}\Delta A$, where ΔA is the difference of surface area. It is known that $E_{vis} \approx \pi\mu D^{1.5}\sigma_{LV}^{0.5}/\rho^{0.5}$, where μ is the water viscosity and ρ is the water density.[23] Exemplified by D = 10 μm, we can obtain $E_s \approx 1 \times 10^{-11}$ J and $E_{vis} \approx 6 \times 10^{-12}$ J. Thus, to ensure the jumping of merged microdrops, the kinetic energy (E_k) must be positive, which means $E_{int} < 4 \times 10^{-12}$ J.

Our previous studies have indicated that surface adhesion of superhydrophobic nanostructures is determined by their geometrical morphologies and solid−liquid contact ways.[24,25] As shown in Figure 4c and d, the retracting and detaching process of microscopic water films on the tops of aligned nanoneedles is governed by the liquid−solid van der Waals attraction[24] and line tension.[26] Accordingly, we can obtain $E_{int} \approx 0.25\pi D^2 \sin^2(\pi - \alpha)(1 + \cos\theta)\sigma_{LV}(d_t/p)^2 + 0.25\pi^2 D^2 \sin^2(\pi$

dx.doi.org/10.1021/jz500798m | J. Phys. Chem. Lett. 2014, 5, 2084−2088

$-\alpha)\tau(d_t/p^2) + \pi^2 D \sin(\pi - \alpha)\tau(d_t/p)$, where α is the apparent contact angle of the condensed microdrop, θ the advanced contact angle of water in contact with the silane modified flat surface (~125°), d_t the top diameter of the nanoneedles, p the interspace, and τ the line tension with the value of $\sim 4 \times 10^{-10}$ J m^{-1} for the top size of ~20 nm (for the detailed deduction, see Supporting Information section S3).[26] Clearly, the E_{int} value is closely related to the top diameter and interspace of the nanoscale building blocks. In this case of d_t = 20 nm and p = 60 nm, the calculated E_{int} is $\sim 3 \times 10^{-13}$ J, which is an order of magnitude lower than the requirement of 10^{-12} J. Therefore, E_{int} is sufficiently low to ensure the efficient self-departure of condensed microdrops with a diameter of ~10 μm, powering by excess surface energy released from their coalescence. Note that the minor inconsistency with experimental findings that a small quantity (<20%) of condensed microdrops with relatively larger diameters (>10 μm) can still be resident on the nanostructure surface should be ascribed to the nonuniformity of characteristic interspaces and top diameters of the as-synthesized ZnO nanoneedles. Besides, our calculation indicated that the contributions of the van der Waals attraction and line tension to E_{int} occupied ~70 and ~30%, respectively. Accordingly, to realize more efficient self-propulsion, ones need to tailor a more delicate structure with reduced d_t and increased p for ensuring the lower adhesion of condensed microdrops in a suspended Cassie state.

In summary, we report a type of closely packed ZnO nanoneedles with efficient self-propelling function of small-scale condensed microdrops, which can be fabricated by very facile, rapid, and inexpensive wet chemical crystal growth followed by hydrophobic treatment. In contrast to the flat surfaces and previous reports, our samples can effectively control the diameters of condensates at the microscale, especially below 10 μm with a drop number distribution of more than 80%. This striking property is ascribed to the minimal solid−liquid adhesion of closely packed nanoneedles, where excess surface energy released from the coalescence of smaller condensed microdrops can be sufficient to ensure the self-propelling of merged microdrops. These findings are significant to develop novel microscale self-propelling dropwise condensation surfaces toward applications in high-efficiency heat transfer devices[1−3] and functional coatings, for example, moisture self-cleaning[27] and subcooled water antifreezing.[28−31]

EXPERIMENTAL METHODS

Sample Preparation. Arrayed ZnO nanoneedles were rapidly synthesized by facile chemical bath deposition. To remove organic contaminants, glass slides with the sizes of 2 cm × 2 cm were first ultrasonically rinsed in acetone, ethanol, and deionized water for 20 min and subsequently dried by N_2 flow. Then, the cleaned glass slides were coated with crystal seeds through dip-coating in an ethanol solution of zinc acetate (0.005 mol L^{-1}) followed by annealing at 350 °C for 20 min, which were repeated three times for obtaining the uniform seeding layers. Aligned nanoneedles were obtained by immersing the seeded glass slides in the aqueous solution of 0.5 mol L^{-1} zinc nitrate hexahydrate and 4 mol L^{-1} sodium hydroxide (V:V = 1:1) at 60 °C for 30 min, where the seeded faces were set downward. After rinsing with water and drying by N_2 flow, all nanostructured samples and contrast glass slides were immersed in the 1.0 wt % ethanol solution of heptadecafluorodecyltrimethoxysilane (Shin-Etsu Chemical Co., Japan) for 2 h at room temperature and then taken out to heat at 80 °C for 1 h.

Structure and Property Characterization. The as-synthesized nanostructures were observed using a high-resolution scanning electronic microscope (Hitachi S4800, Japan). The high-speed charge-coupled device camera (CCD) of the Motion Analysis Microscope system (Keyence VW-9000, Japan) was used for observing the rapid behaviors of microdrops under magnifications of 30−1000× with frame rates of 30−4000 fps. The samples were fastened on the cooling stage (~1 °C) at the controlled environment of an ambient temperature of 25 °C and relative humidity of ~90%. The sample stage, CCD, and light source were set coaxially in the optic path, where the CCD holder could be rotated for capturing the top views, tilted views, and side views of optical images and video. A special measure using optical grating structure films as substrates and 45°-tilted illumination was used for capturing the images in Figures 2, S1, and S2 (Supporting Information), which enhance the stereoscopic and colorful effects of condensed microdrops to highlight the distinction of two condensation modes.

ASSOCIATED CONTENT

Supporting Information

Detailed dropwise condensation dynamics on the vertically placed flat surface (Figure S1) and the horizontally placed nanostructured surface (Figure S2) and detailed deduction of interfacial adhesion-induced dissipation energy (section S3) are included. This material is available free of charge via the Internet at http://pubs.acs.org.

AUTHOR INFORMATION

Corresponding Author

*E-mail: xfgao2007@sinano.ac.cn.

Notes

The authors declare no competing financial interest.

ACKNOWLEDGMENTS

This work was supported by the National Basic Research Program of China (2012CB933202, 2012CB934101, 2013CB933033), the Key Research Program of the Chinese Academy of Sciences (KJZD-EW-M01), and SINANO, CAS.

REFERENCES

(1) Boreyko, J. B.; Zhao, Y. J.; Chen, C.-H. Planar Jumping-Drop Thermal Diodes. *Appl. Phys. Lett.* **2011**, *99*, 234105.
(2) Miljkovic, N.; Wang, E. N. Condensation Heat Transfer on Superhydrophobic Surfaces. *MRS Bull.* **2013**, *38*, 397−406.
(3) Miljkovic, N.; Enright, R.; Wang, E. N. Modeling and Optimization of Superhydrophobic Condensation. *J. Heat Transfer* **2013**, *135*, 111004.
(4) Chen, C.-H.; Cai, Q.; Tsai, C.; Chen, C.-L.; Xiong, G.; Yu, Y.; Ren, Z. Dropwise Condensation on Superhydrophobic Surfaces with Two-Tier Roughness. *Appl. Phys. Lett.* **2007**, *90*, 173108.
(5) Dorrer, C.; Rühe, J. Wetting of Silicon Nanograss: From Superhydrophilic to Superhydrophobic Surfaces. *Adv. Mater.* **2008**, *20*, 159−163.
(6) Miljkovic, N.; Enright, R.; Wang, E. N. Effect of Droplet Morphology on Growth Dynamics and Heat Transfer during Condensation on Superhydrophobic Nanostructured Surfaces. *ACS Nano* **2012**, *6*, 1776−1785.
(7) Enright, R.; Miljkovic, N.; Al-Obeidi, A.; Thompson, C. V.; Wang, E. N. Condensation on Superhydrophobic Surfaces: The Role of Local Energy Barriers and Structure Length Scale. *Langmuir* **2012**, *28*, 14424−14432.

(8) Miljkovic, N.; Preston, D. J.; Enright, R.; Wang, E. N. Electrostatic Charging of Jumping Droplets. *Nat. Commun.* **2013**, *4*, 2517.
(9) Dietz, C.; Rykaczewski, K.; Fedorov, A. G.; Joshi, Y. Visualization of Droplet Departure on a Superhydrophobic Surface and Implications to Heat Transfer Enhancement during Dropwise Condensation. *Appl. Phys. Lett.* **2010**, *97*, 033104.
(10) Feng, J.; Qin, Z.; Yao, S. Factors Affecting the Spontaneous Motion of Condensate Drops on Superhydrophobic Copper Surfaces. *Langmuir* **2012**, *28*, 6067−6075.
(11) Feng, J.; Pang, Y.; Qin, Z.; Ma, R.; Yao, S. Why Condensate Drops Can Spontaneously Move Away on Some Superhydrophobic Surfaces but Not on Others? *ACS Appl. Mater. Interfaces* **2012**, *4*, 6618−6625.
(12) Enright, R.; Miljkovic, N.; Dou, N.; Nam, Y.; Wang, E. N. Condensation on Superhydrophobic Copper Oxide Nanostructures. *J. Heat Transfer* **2013**, *135*, 091304.
(13) Miljkovic, N.; Enright, R.; Nam, Y.; Lopez, K.; Dou, N.; Sack, J.; Wang, E. N. Jumping-Droplet-Enhanced Condensation on Scalable Superhydrophobic Nanostructured Surfaces. *Nano Lett.* **2012**, *13*, 179−187.
(14) Chen, X.; Wu, J.; Ma, R.; Hua, M.; Koratkar, N.; Yao, S.; Wang, Z. Nanograssed Micropyramidal Architectures for Continuous Dropwise Condensation. *Adv. Funct. Mater.* **2011**, *21*, 4617−4623.
(15) Rykaczewski, K.; Paxson, A. T.; Anand, S.; Chen, X.; Wang, Z.; Varanasi, K. K. Multimode Multidrop Serial Coalescence Effects during Condensation on Hierarchical Superhydrophobic Surfaces. *Langmuir* **2013**, *29*, 881−891.
(16) Boreyko, J. B.; Chen, C.-H. Self-Propelled Dropwise Condensate on Superhydrophobic Surfaces. *Phys. Rev. Lett.* **2009**, *103*, 184501.
(17) He, M.; Zhang, Q.; Zeng, X.; Cui, D.; Chen, J.; Li, H.; Wang, J.; Song, Y. Hierarchical Porous Surface for Efficiently Controlling Microdroplets' Self-Removal. *Adv. Mater.* **2013**, *25*, 2291−2295.
(18) Tian, J.; Zhang, Y.; Zhu, J.; Yang, Z.; Gao, X. Robust Nonsticky Superhydrophobicity by the Tapering of Aligned ZnO Nanorods. *ChemPhysChem* **2014**, *15*, 858−861.
(19) Beysens, D. The Formation of Dew. *Atmos. Res.* **1995**, *39*, 215−237.
(20) Nam, Y.; Kim, H.; Shin, S. Energy and Hydrodynamic Analyses of Coalescence-Induced Jumping Droplets. *Appl. Phys. Lett.* **2013**, *103*, 161601.
(21) Peng, B.; Wang, S.; Lan, Z.; Xu, W.; Wen, R.; Ma, X. Analysis of Droplet Jumping Phenomenon with Lattice Boltzmann Simulation of Droplet Coalescence. *Appl. Phys. Lett.* **2013**, *102*, 151601.
(22) He, M.; Zhou, X.; Zeng, X.; Cui, D.; Zhang, Q.; Chen, J.; Li, H.; Wang, J.; Cao, Z.; Song, Y.; et al. Hierarchically Structured Porous Aluminum Surfaces for High-Efficient Removal of Condensed Water. *Soft Matter* **2012**, *8*, 6680−6683.
(23) Chandra, S.; Avedisian, C. T. On the Collision of a Droplet with a Solid Surface. *Proc. R. Soc. London, Ser. A* **1991**, *432*, 13−41.
(24) Lai, Y.; Gao, X.; Zhuang, H.; Huang, J.; Lin, C.; Jiang, L. Designing Superhydrophobic Porous Nanostructures with Tunable Water Adhesion. *Adv. Mater.* **2009**, *21*, 3799−3803.
(25) Gao, X.; Yao, X.; Jiang, L. Effects of Rugged Nanoprotrusions on the Surface Hydrophobicity and Water Adhesion of Anisotropic Micropatterns. *Langmuir* **2007**, *23*, 4886−4891.
(26) Wong, T.-S.; Ho, C.-M. Dependence of Macroscopic Wetting on Nanoscopic Surface Textures. *Langmuir* **2009**, *25*, 12851−12854.
(27) Wisdom, K. M.; Watson, J. A.; Qu, X.; Liu, F.; Watson, G. S.; Chen, C.-H. Self-Cleaning of Superhydrophobic Surfaces by Self-Propelled Jumping Condensate. *Proc. Natl. Acad. Sci. U.S.A.* **2013**, *110*, 7992−7997.
(28) Chen, X.; Ma, R.; Zhou, H.; Zhou, X.; Che, L.; Yao, S.; Wang, Z. Activating the Microscale Edge Effect in a Hierarchical Surface for Frosting Suppression and Defrosting Promotion. *Sci. Rep.* **2013**, *3*, 2515.
(29) Yao, X.; Song, Y.; Jiang, L. Applications of Bio-Inspired Special Wettable Surfaces. *Adv. Mater.* **2011**, *23*, 719−734.
(30) Boreyko, J. B.; Collier, C. P. Delayed Frost Growth on Jumping-Drop Superhydrophobic Surfaces. *ACS Nano* **2013**, *7*, 1618−1627.
(31) Zhang, Q.; He, M.; Chen, J.; Wang, J.; Song, Y.; Jiang, L. Anti-Icing Surfaces Based on Enhanced Self-Propelled Jumping of Condensed Water Microdroplets. *Chem. Commun.* **2013**, *49*, 4516−4518.